

Study of a large landslide and mudflow at Gaspar, SC, Brazil

Marcelo Heidemann & Luiz A. Bressani
*Department of Civil Engineering – Federal University of Rio Grande do Sul,
Porto Alegre/RS, Brazil*
Juan A. Altamirano Flores
*Department of Geosciences – Federal University of Santa Catarina,
Florianópolis/SC, Brazil*



ABSTRACT

In November 2008 after a 56 days long rainy period the North of Santa Catarina state suffered a severe rainstorm (450mm/2 days). The paper describes the studies that have been carried out on an extremely fast landslide which happened a week after this rainstorm. The slide involved a granulate residual soil which was classified as inorganic sandy silt but that showed large packets of kaolinite minerals. Its hydraulic conductivity was of the order of 5×10^{-8} m/s. Triaxial, direct shear and ring shear tests have been carried out on the soil. Although in the back-analysis of the initial failure the peak shear strength was necessary to properly explain the slide, the liquefaction that followed was probably caused by a drop from peak to residual shear strength due to re-alignment of the clay particles.

RESUMEN

En noviembre de 2008 después de 56 días de lluvias, el norte del estado de Santa Catarina fue afectado por severas precipitaciones (450 mm / 2 días). Este artículo presenta los estudios realizados en un deslizamiento de tierra muy rápido ocurrido una semana después del periodo de lluvias intensas. El deslizamiento de tierra corresponde a un suelo residual que se clasifica como un silte inorgánico con arena, que presentó grandes agregados de caolinita. Su conductividad hidráulica es del orden de 5×10^{-8} m/s. En este suelo fueron realizados ensayos triaxial y de corte directo. Aunque en el retro análisis de la ruptura inicial la resistencia al corte de pico explicaría mejor el deslizamiento, todavía la licuefacción que se siguió fue causada, probablemente por reducción para la resistencia al corte residual debido al re-alineamiento de las partículas de arcillas.

1 INTRODUCTION

In November 2008 the Itajaí Valley at Santa Catarina state, Brazil, was subjected to a rainy season that lasted about 56 days. After this period there was a short period of high intensity rainfall (about 450mm in two days in some spots).

These rains triggered a series of landslides that killed 135 people and destroyed homes, roads, power transmission systems and communication networks and other lifelines. The severe damage caused by this episode led to studies in the area in an effort to understand the mechanisms that led to the initiation of mass movements.

This work describes the study of an extremely fast large rotational landslide which occurred a week after the occurrence of heavy rains in the city of Gaspar – SC. The landslide mobilized a volume of approximately 110,000 m³ of residual soil of granulate and caused the deaths of two people.

The geotechnical characterization and tests to define shear strength parameters have been carried out on the residual soil involved in the landslide. Hydraulic conductivity tests were also done on undisturbed soil samples collected from the site.

2 REVIEW ON RAINFALL AND MASS MOVEMENTS

The rains have an intimate relationship with mass movements and are pointed as the main cause of instability of slopes in various parts of the world (Gulla et al. 2008; Ocakoglu et al. 2001; Hawke and McConchie, 2003; van Asch et al. 1999).

This relationship is even greater in tropical and subtropical regions, which are constantly affected by weather phenomena that cause heavy rains with long duration, such as tropical storms and monsoons (Alcantara-Ayala, 2003, Chen et al. 2006; Dahal and Hasegawa, 2008; Gabet et al. 2004; Leroueil, 2001, Miller et al. 2009; Saito et al. 2010; Tohari et al. 2007; Zhou et al. 2002). In Brazil the heavy rainfalls are also considered the main trigger of mass movements (Ahrendt and Zuquette, 2003).

De Vita and Reichenbach (1997) present a list with references to more than 450 studies about mass movements induced by rainfalls, with geotechnical, geological, hydrological and geomorphological approaches about the problem.

On the other hand, Zhou et al. (2002) and Guidicini and Nieble (1984), argue that are few studies carried out to establish a relationship between rainfall and mass movements in natural surroundings, mainly due to the lack of data related to the moment of failure.

There is great discussion on the literature about the relationship between intensity and duration of rain which

cause mass movements. There are different conclusions about the role of previous rainfall on the effect of an intense storm which caused instability (Morgenstern, 1992 *apud* Rahardjo et al. 2001; Rahardjo et al. 2007).

The triggering mechanisms of landslides by rainfall is related, in general terms, to the volume and intensity of rainfall and soil hydraulic conductivity, which is governed by the size and arrangement of mineral soils, mainly influenced by the upper layers as a low permeability leads to increased surface runoff (Høydal and Heyerdahl, 2006). Therefore, on slopes with low permeability surface soils, heavy rainfall will have little effect on its stability since only a portion of the rainfall will seep into the soil. These slopes are more affected when rainfall precipitates during prolonged periods, usually with less intensity.

However, on slopes with soils of high permeability, most of the precipitated water during heavy rainfalls may infiltrate into the ground, which leads to rapid variations of pore pressures and of the stability factor. In these materials the rains of low intensity, even for long periods, have little effect, since the drainage of infiltrated water is also fast (Rahardjo et al. 2001 and Bressani et al. 2009).

Quite often the failures occur with a time lag in relation to the rains that cause them. According to Leroueil (2001), this occurs because the changes in pore pressures at greater depths are delayed compared with the changes that occur near the surface. Analyzing mass movements which occurred in the town of Campos do Jordão, Ahrendt and Zuquette (2003) found that some mass movements did not occur during the rains, but some time later. They also came to the conclusion that for that occasion the rainfall distribution played a more important role than its quantity.

3 CHARACTERIZATION OF THE RAINFALL AND MASS MOVEMENT

The mass movement studied occurred at Belchior Baixo, Gaspar - SC, Brazil. The map of Figure 1 shows the location of the town.



Figure 1. Location of the town

In 2008 the SC state recorded a rainy season that began in mid-August and extended until the end of

November, with almost daily rains for about three and a half months, especially in the Itajaí Valley.

According to Flores et al. (2009), the peak of the rainfall was the result of an atmospheric condition where the circulation of the Atlantic Ocean east winds caused winds at low levels in the atmosphere since November 19, 2008. This atmospheric instability was reinforced on November 21 to 23 by a Cyclonic Vortex, also at mid levels of the atmosphere, causing concentrated rainfalls in the Itajaí Middle Valley.

The peak of the rains occurred during four days (21 and 25 November 2008), with recorded cumulative values exceeding 500 mm in Blumenau and almost 700 mm in neighboring towns of Luiz Alves and Gaspar.

The instability studied is situated in a range of small elevations, where occurs the contact between the geological units called "Complex Luis Alves", characterized by granulitic/gneissic rocks, and the "Itajaí Group", consisting of conglomerates, sandstones and other sedimentary materials.

The hot and humid climate, coupled with the age of the granulitic rocks (Archean-Paleoproterozoic) led to the development of a thick soil profile, which in the site is greater than 15m.

During the torrential rains of 22 and 23 November two lateral slides involving the local conglomerates occurred in the same area. The disruptions were of low speed (about 2-4m/h according to witnesses), having destroyed a residence but causing no victims.

It was only on December 6th that the 2 main movements occurred. The first, classified as a fast rotational sliding of wet soil (Cruden and Varnes criterion, 1996), was followed almost immediately by a great mass movement in the form of an extremely fast rotational sliding of wet soil, followed by very rapid mud and debris flow. This big slide moved a volume of soil estimated at 110,000 m³ (estimate based on the method proposed by Cruden and Varnes, 1996). The resulting scar of the movement is shown in Figure 2 (February 2010). Figure 3 shows an aerial view of the area of instability (on the left) and an older scar close by.



Figure 2. The scar of the movement – photo of February 2010.

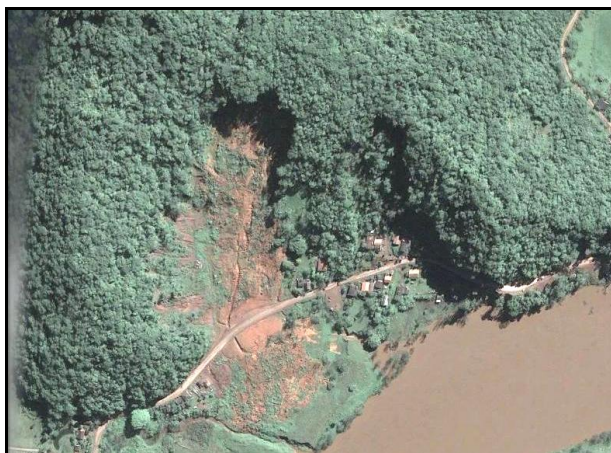


Figure 3. Satellite view of the landslide area (left scar) – image date: 03/08/2009, Google Earth.

4 METHODOLOGY

This work carried out the geotechnical characterization, through laboratory testing, of the residual soil of granulite involved in the mass movement described.

4.1 Soil sampling

Undisturbed samples of soil were taken from the main scar left by the movement. The soil samples were carefully carved in the form of blocks with 12-15cm in diameter and 20-25 cm height. Samples were also collected with the use of metal rings for direct shear tests (6 cm in diameter).

4.2 Tests of hydraulic conductivity

Two types of tests to determine the coefficient of hydraulic conductivity (k_{sat}) have been carried out, one in a permeameter of flexible walls and mercury column with confining pressures of 25, 50, 100, 200 and 400 kPa. A hydraulic gradient of about 35 was used. The second set of tests was conducted in the conventional triaxial equipment during CID-U tests (see below), with k_{sat} being measured before and after peak of the shearing tests using confining pressures of 50, 100 and 200 kPa. To promote the flow of water through the soil, a pressure difference of about 10 kPa between top and bottom of the specimen was used (a hydraulic gradient equal to 10).

4.3 Shearing strength tests

4.3.1 Triaxial tests

The triaxial tests performed were aimed at determining the soil shear strength under undrained conditions and when subjected to a stress path that would simulate the increase in pore pressure by rain on slopes.

The triaxial tests were conducted using confining stresses of 50, 100 and 200 kPa. The undisturbed specimens with 100 mm in height and 50 mm in diameter were cut from small blocks of soil collected in the field.

Remolded specimens of the same dimensions were prepared by static compaction of soil using a press and a metal mold, as proposed by Brenner (1985).

The remolded specimens were subjected to CIU tests. In undisturbed samples were run CID-U type tests, using special stress paths such as those employed by Bressani and Vaughan (1989) and Futai et al. (2004), aimed to investigate the behaviour of structured soils (Figure 4).

This stress path seeks to simulate the behavior of the soil on slopes in the destabilization process under rainfall. The techniques for specimen saturation by backpressure and for consolidation were identical to those performed in the CIU tests. In these tests the hydraulic conductivity were also measured after the consolidation and after the peak (failure).

The conventional loading drained stage was carried out until reaching levels of shear stress of about 80% of the estimated failure stress (based on direct shear tests results). At that level, the shear stress was kept constant and the test continued with the steady increase in pore pressure up to failure (see Figure 4). Once the failure was well-defined, the drainage was closed and the specimen was deformed furthermore under undrained conditions, so allowing the definition of the shear strength envelope in the region. Area correction of the specimens was used to calculate the results as proposed by La Rochelle et al. (1988).

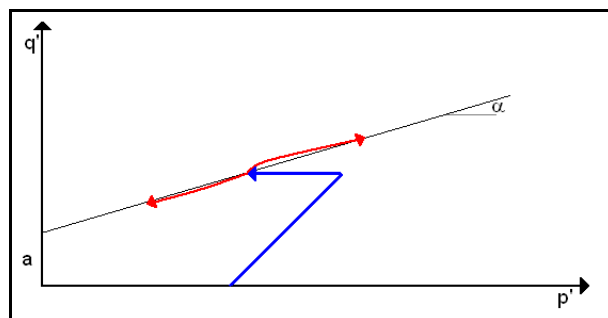


Figure 4. Effective stress path used on CID-U tests

4.3.2. Ring shear tests

In order to define the parameters of residual strength of the residual soil of granulite, ring shear tests were performed on equipment originally described by Bromhead (1979). The tests were performed with normal stresses of 50, 100, 200 and 400 kPa, adopting a single stage, i.e. for each stress level one specimen was tested. After mounting the specimen a pre-shearing was done in order to reach the residual condition faster (Anayi et al. 1988; Stark and Vettel, 1992). The rate used during the tests was approximately $0.12^\circ / \text{min}$ ($0.089 \text{ mm} / \text{min}$) which was suggested by Pinheiro et al. (1997).

4.4 Microstrutural studies

The investigation of the microstructural aspects of the soil was made through X-ray diffraction and scanning electron microscopy. Analyses were performed on oriented, natural, glycolated and calcined powdered samples.

5 RESULTS

5.1 Physical characterization

Table 1 shows the composition of the soil particle size, obtained with and without the use of dispersant. The soil consists of inorganic silt with sand (ML).

The use of dispersant shows a considerable portion of clay that otherwise could be either (i) stuck together in silt-size clumps or (ii) lightly bonded with larger particles. The clay particles account for about 15% of the soil composition and have normal activity ($A_c = 1.03$).

The Atterberg limits were determined on air-dried samples and from natural moisture. In both samples the results were similar, with the soil in natural state having $LL = 49\%$ and $IP = 18.5\%$, while the air dried sample have $LL = 47\%$ and $IP = 16$.

Table 2 presents the physical indices obtained from undisturbed samples used in laboratory tests.

Table 1. Soil grading (with and without the use of dispersant)

	With dispersant (%)	Without dispersant (%)
Gravel	0	0
Coarse sand	0	0
Medium sand	1,92	1,73
Fine sand	18,75	19,81
Silt	63,87	78,09
Clay	15,46	0,37

Table 2. Indexes of the soil.

	Average	Standard deviation
w_{nat} (%)	39,75	1,46
G_s (kN/m ³)	25,97	-
γ_{nat} (kN/m ³)	16,63	0,37
γ_d (kN/m ³)	11,90	0,35
S_r (%)	86,84	1,75
e	1,21	0,03
η	0,55	0,01

5.2 Hydraulic conductivity

In Figure 5 are presented the coefficients of hydraulic conductivity (K_s) obtained from tests in the triaxial compression chamber and in the permeameter.

The coefficient of hydraulic conductivity measured at different confining stresses showed a well-defined reduction in the k_{sat} coefficient with increasing confining stress. The value of k_{sat} was found to be within the range of silty soils.

The results obtained before and after shearing in triaxial tests show that there is a slight reduction in hydraulic conductivity after the failure and associated deformations. In the test with confining pressure of 50 kPa this variation was more pronounced than in higher pressures.

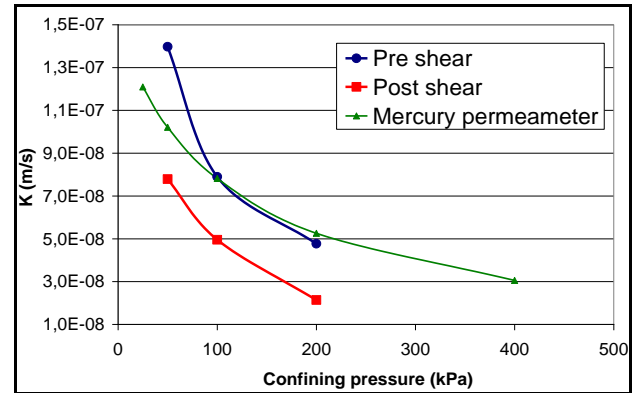


Figure 5. Hydraulic conductivity tests results

5.3 Shearing strength

5.3.1. Ring shear

The ring shear tests were executed with the objective of determining the residual shear strength of this residual soil of granulite. Figure 6 shows the stress-strain curves obtained in these tests. From these results an almost straight line defines a residual angle of internal friction of 8.8° .

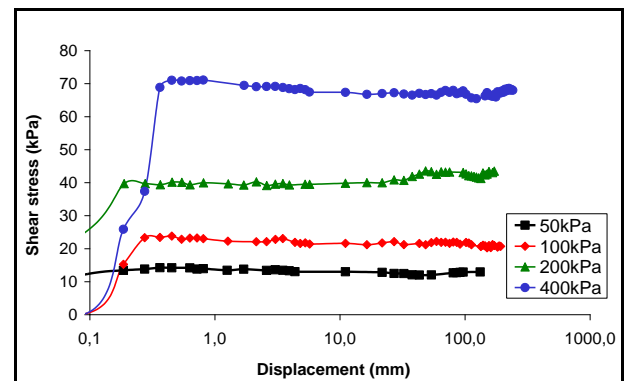


Figure 6. Stress displacement curves obtained from ring shear tests

This value of $\phi'_r = 8.8^\circ$ is quite low when compared to those obtained in several Brazilian tropical soils. However, according to data presented by Rigo et al. (2006) (Figure 7), the residual soil of granulite is similar to some soils composed of partially weathered minerals, as they present low residual friction angle in spite of their low IP. According to Rigo et al. (2006), this is due to degradation of the partially weathered minerals when subjected to large shear strains, with subsequent orientation of the particles and so promoting failure under transitional or even sliding conditions.

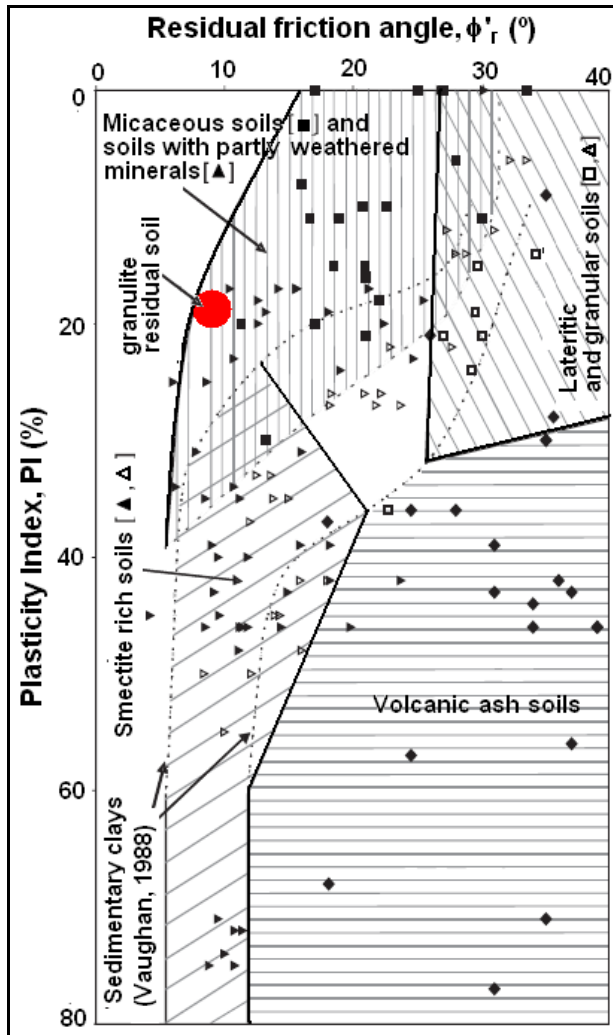


Figure 7. Graph of plasticity index versus residual friction angle for tropical soils showing results of this work (modified from Rigo et al. 2006)

5.3.2 Triaxial tests

The results of CIU triaxial tests on remolded specimens are shown in Figures 8 and 9. The first presents the stress- strain curves and the second the effective stress paths found.

The effective stress path test with $\sigma_c = 50$ kPa shows a typical behavior of dense materials (due to compaction), with clear curvature to the right. The tests with $\sigma_c = 100$ kPa and 200 kPa show changing behaviors with greater tendency to the vertical or even to the left of the graph. It is interesting to observe that the TTE of the 3 tests reaches a well defined straight envelope of failure (kf line).

Figure 10 shows the main results obtained from the special CID-U triaxial tests (stress-axial strain and volumetric strain – axial strain) and Figure 11 shows the effective stress paths (ESP) partly induced on the specimens (see methodology above).

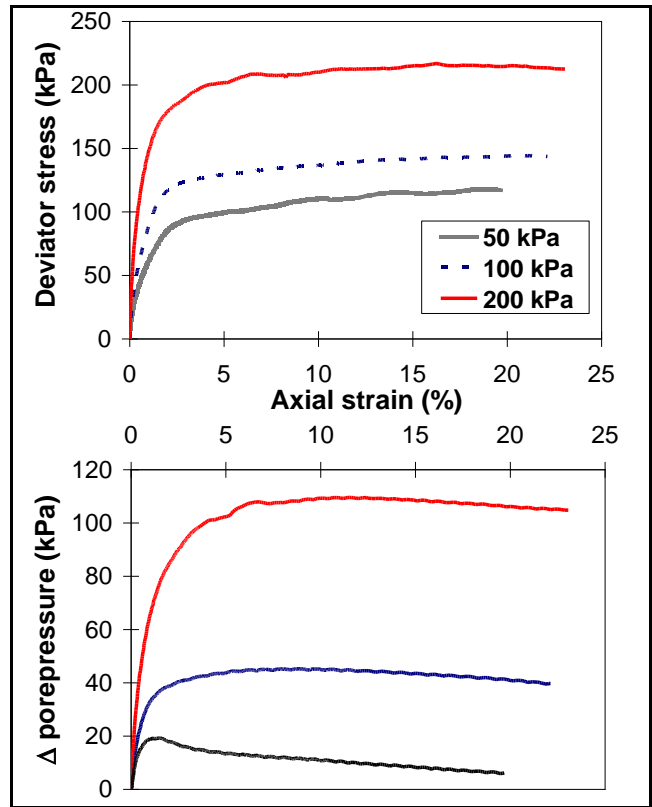


Figure 8. Deviator stress and pore-pressure versus axial strain curves obtained on CIU triaxial tests on remolded specimens

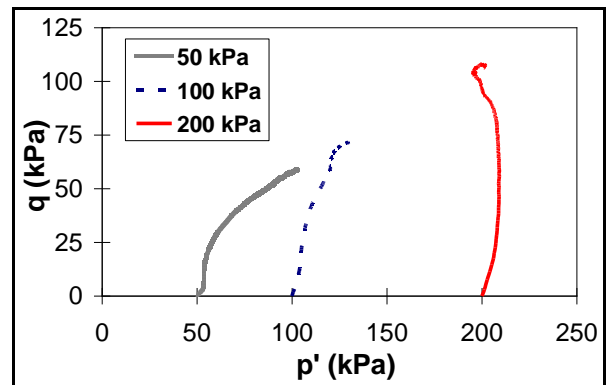


Figure 9. Effective stress paths obtained on CIU triaxial tests on remolded specimens

The ESP obtained in the final non-drained stage of the tests showed a distinct behavior for the three specimens. For test with $\sigma_c = 50$ kPa there was a sharp gain of resistance leading to values of p' close to 100 kPa and $q = 70$ kPa and showing q increase even after 20% of axial strain. For test with $\sigma_c = 100$ kPa the stage of undrained shearing resulted in an increase of p' and q , but the increase reached a maximum for $q = 80$ kPa followed by a steadily decrease in shear stress. For the test with $\sigma_c = 200$ kPa, the undrained stage seemed to

cause little variation the shear stress even after quite large axial strains.

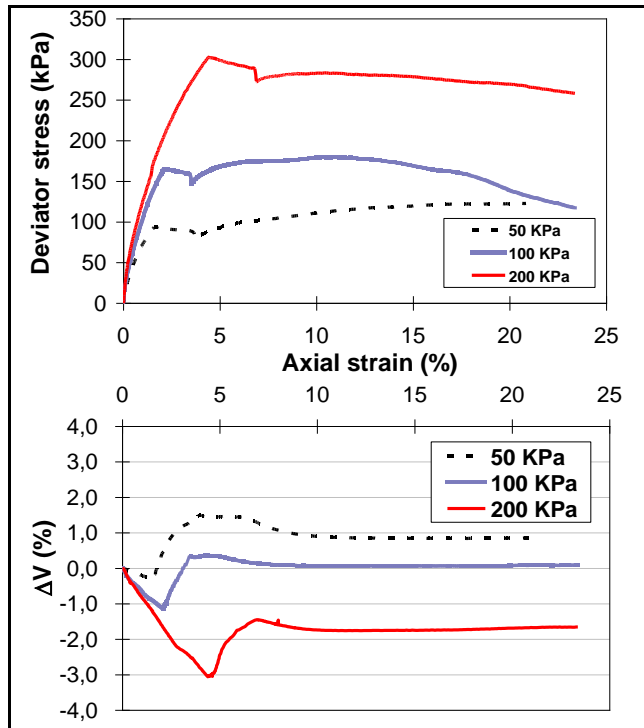


Figure 10. Deviator stress and volumetric strain versus axial strain on special CID-U tests

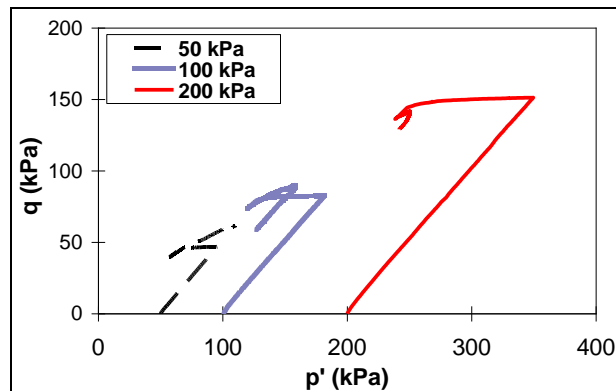


Figure 11. Effective stress paths followed by the special CID-U tests on undisturbed specimens

In these tests during the stage of pore pressure increase there was a slightly tendency to reduce the shear strength, until close to failure, when there was a clear drop of shear stress. The amount of axial strain up to this point varied depending of the confining stress applied (2-5%).

Table 3 presents the shear strength parameters derived from the triaxial tests on the soil. It is interesting to note that the shear strength parameters were little affected by the two types of specimens.

Table 3. Shear strength parameters derived from triaxial tests on undisturbed and remolded soil.

Test and soil condition	ϕ'	c'
CID-U test – undisturbed	32,3	12,5
CIU test – remolded	29,5	9,8

5.4 Analyses of microstructures

A first aspect observed in the analysis of X-ray diffraction was the occurrence of a peak related to the presence of smectite in the sample powder which however did not appear in the samples oriented and glycolated. Although the tests were repeated the same results were obtained. This phenomenon may be caused by the fact that the smectite in this soil is present in a finer fraction, probably smaller than 2 μm , which is used as a standard in the analysis of x-ray diffraction on aligned samples. For such reason these clay minerals could be found only in natural sample analysis.

The clay fraction of this soil presents a predominance of kaolinite, with its occurrence observed even by visual inspection of the soil. Illite, montmorillonite, plagioclase and quartz are also present in smaller quantities.

It is noteworthy that the size of the kaolinite lumps observed in the SEM usually had more than 2 μm in length which led them to be classified as silts in the grading tests. However, when these particles are broken due to intense handling or due to shearing stresses (lab or field), they will reduce to clay-size lamellar particles, behaving like real clays.

Figure 12 is a photograph of a kaolinite lump in the soil showing its structural peculiarities (image obtained by SEM).

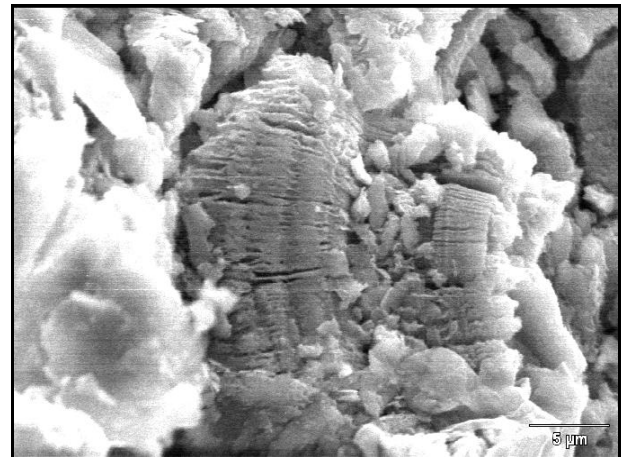


Figure 12. Photograph of kaolinite lump found in the soil (2000x original amplification)

6 STABILITY ANALYSIS

Using the determined geotechnical parameters of the soil, slope stability analysis were carried out. The analysis

used limit equilibrium software SlopeW (modified Bishop and Morgenstern-Price methods).

Some conditions and assumptions were assumed to perform these trials:

- two cross-sections of the slope were analyzed, based on a topographical map produced by Flores et al. (2009);
- because of the long previous rainy season (about 62 days), it was assumed that the suction was negligible by the date of failure;
- as the inspection of the slope scar showed no outcrop of bedrock, it was assumed that failure involved only the granulite residual soil;
- the peak shear strength parameters obtained from undisturbed specimens were used (CID-U triaxial tests; $\phi' = 32.3$ and $c' = 12.5$ kPa).

A number of simulations were carried out to analyze the consistency of shear strength parameters obtained in the laboratory with the back-analysis considering a failure surface similar with that observed in the field. The retro-analysis aimed to find what was the water level leading a FS = 1 with the failure surface geometry similar to that observed in the field.

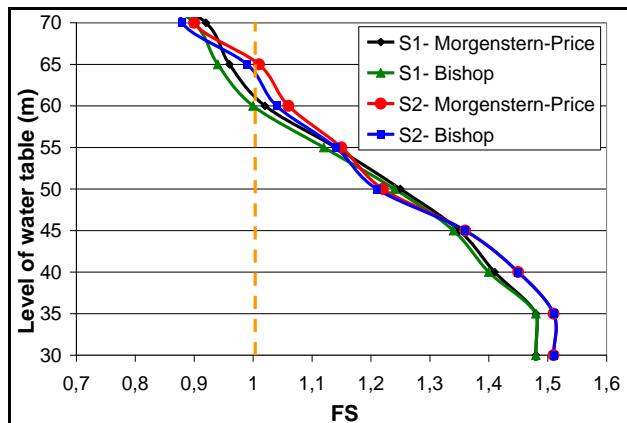


Figure 13. Factors of safety in relation to the water level inside the slope (SlopeW results)

Figure 13 shows the FS as a function of the adopted water level. In the figure is clear the small difference between both methods of analysis. As the water level was increased from 35 m, the FS reduced almost linearly reaching the value of 1 around 59m. In this condition the obtained failure surface was in agreement with the observed field geometry.

It is interesting to note that when trying to perform these simulations using shear strength parameters of large deformations (or residual condition) the FS drop to values close to 0.5, even without the water level. This shows that when the stability of the slope is influenced by these parameters, which may occur after a certain level of straining, the slope will present a major reduction in its stability condition. Such reduction on stability condition could induce the very quick failure reported by the eye witnesses.

7 DISCUSSION AND CONCLUSIONS

The granulite residual soil involved in the movement is classified as inorganic silt with sand. However the X-Ray diffraction studies and electron microscopy revealed the occurrence of clays that are not detectable in conventional particle size analysis, even with the use of dispersant agent. The reason is that many clay particles are arranged in packets of silt-size (probably due to incomplete weathering).

The granulite soil has low hydraulic conductivity, with typical values of silts ($k = 1 \times 10^{-7}$ to 3×10^{-8} m/s). After failure by shearing in triaxial tests, the soil showed a reduction of about two times of the hydraulic conductivity (perpendicular to the plane of failure). In the field, such characteristic can give rise to the appearance of low permeability zones and the consequent increase in pore pressures. Such low permeability may have contributed to the observed delay of about one week between the intense rainfall episodes and time of sliding.

Using results of triaxial CID-U it was possible to verify the influence of elevation of pore pressure in this soil. Close to failure, the tendency to reduce the shear stress was very marked, and difficult to maintain the specified value. This may indicate a certain degree of soil brittleness.

Stability analyses were performed based on parameters obtained from laboratory tests (peak resistance of triaxial tests). Although no complete profiles of the slope were available or information on previous water level, the simulations showed the consistency of the shear strength parameters used.

The stability analyses using the reconstructed topography showed that the FS of the slope becomes very close to 1 when the water level reaches the elevation 59m.

As the soil of granulite has packages of lamellar particles (observed by electron microscopy), during shearing these particles suffer a marked textural change resulting in individual clay particles. This lamellarity gives a characteristic to the soil that leads to the development of residual strength (Stark and Eid, 1994). The results of direct shear tests indicate that the peak strength reduction leading to the residual value is relatively fast. The ring-type shear tests indicated that the residual angle of internal friction is $\phi'_r = 8.8^\circ$.

It is interesting to note that, if the soil starts to behave in a residual shear strength condition after some straining, the stability calculations indicated that the slope will be in over critical condition, causing a very quick failure. According to reports of witnesses that was the kind of failure observed, with no previous signs, such as cracks or displacements, prior to the sliding.

ACKNOWLEDGEMENTS

The authors thank CNPq and CAPES for encouraging this research and for providing individual research grants for two authors.

Analyses of scanning electron microscopy (SEM) were performed at the Center for Electron Microscopy at

UFRGS. The diffraction of X-rays was performed at the Laboratory of X-ray diffraction at UFRGS.

Field studies were supported by the Department of Geosciences from Philosophy and Humanities Center at the Universidade Federal de Santa Catarina.

REFERENCES

- Ahrendt, A. and Zuquette, L.V. 2003. Triggering factors of landslides in Campos do Jordão, Brazil. *Bull. Eng. Geol. and Environ.*, 62: 231-244.
- Alcantara-Ayala, I. 2004. Hazard assessment of rainfall-induced landsliding in Mexico. *Geomorphology*, 61: 19-40.
- Anayi, J.T. et al. 1988. Comparison of alternative methods of measuring the residual strength of a clay. *Transportation Research Board*, Washington, D.C., USA.
- Brenner, R.P. et al. 1985. Field stress path simulation of rain-induced slope failure. Proc. 11th Int. Conf. on Soil Mechanics. and Found. Eng. A.A. Balkema, Brookfield, USA.
- Bressani, L. A., and Vaughan, P. R. 1989. Damage to soil structure during triaxial testing. 12th Int. Conf. Soil Mech. and Found. Eng., v.1, Rio de Janeiro, Brazil.
- Bressani, L. A. et al. 2009. Análise de um Ruptura de Talude Íngreme em Solo Coluvionar de São Vendelino, RS. 5^o COBRAE, v.1, ABMS, São Paulo, Brasil.
- Bromhead, E. N. 1979. A simple ring shear apparatus. *Ground Engineering*, 12(5): 40-44.
- Chen, H. et al. 2006. Recent rainfall-induced landslides and debris flow in northern Taiwan. *Geomorphology*, 77: 112-125.
- Cruden, D.M. e Varnes, D.J. 1996. Landslide types and processes. *Landslides: Investigation and Mitigation* (A.K. Turner e R.L. Schuster, eds.), TRB, National Research Council, Washington, D.C. USA.
- Dahal, R.K. e Hasegawa, S. 2008. Representative rainfall thresholds for landslides in the Nepal Himalaya. *Geomorphology*, 100: 429-443.
- De Vita, P. and Reichenbach, P. 1998. Rainfall-triggered landslides: a reference list. *Environ. Geol.*, 35: 219-233.
- Flores, J.A.A. et al. 2009. Movimentos gravitacionais de massa no município de Gaspar, Vale do Itajaí, SC, na catástrofe de novembro de 2008. 13^o Simp. Bras. Geog. Física e Aplic. Viçosa, Brasil. Available. in: www.geo.ufv.br/simposio/simposio/trabalhos
- Futai, M.M. et al. 2004. Yield, Strength, and Critical State Behavior of a Tropical Saturated Soil. *J. of Geotech. and Geoenv. Eng.*, 130(11): 1169-1179.
- Gabet, E. J. et al. 2004. Rainfall thresholds for landsliding in the Himalayas of Nepal. *Geomorphology*, 63: 131-143.
- Guidicini, G. e Nieble, C.M. 1984. *Estabilidade de taludes naturais e de escavação*. Edgard Blücher, São Paulo, Brasil.
- Gullà, G. et al. 2008. Susceptibility and triggering scenarios at a regional scale for shallow landslides. *Geomorphology*, 99: 39-58.
- Hawke, R. M. and MC Conchie, J. A. Variability of in situ moisture measurements and implications for modeling hillslope processes. *Env. & Eng. Geoscience*, 9: 213-223.
- Høydal, Ø.A. and Heyerdahl, H. 2006. Methodology for calculation of rain-induced slides. *Unsaturated Soils*, 473-484.
- La Rochelle, P. et al., 1988. Observational approach to membrane and area corrections in triaxial tests. *Advanced Triaxial Testing of Soil and Rock*. Philadelphia, USA.
- Leroueil, S. 2001. Natural slopes and cuts: movement and failure mechanisms. *Géotechnique*, 51(3): 197-243.
- Miller, S. et al. 2009. Rainfall thresholding and susceptibility assessment of rainfall-induced landslides: application to landslide management in St Thomas, Jamaica. *Bull. of Eng. Geol. and Env.*, 68: 539-550.
- Ocakoglu, F. et al. 2002. Dynamics of a complex mass movement triggered by heavy rainfall: a case study from NW Turkey. *Geomorphology*. 42: 329-341.
- Pinheiro, R.J.B. et al. 1997. A study on the residual shear strength of two unstable slopes in the state of Rio Grande do Sul. Pan-American Symp. Landslides, COBRAE, v.1. Rio de Janeiro, Brazil.
- Rahardjo, H. et al. 2007. Factors Controlling Instability of Homogeneous Soil Slopes under Rainfall. *J. Geotech. and Geoenv. Eng.*, 133(12): 1532-1543.
- Rahardjo, H. et al. 2001. The effect of antecedent rainfall on slope stability. *Geotech. and Geol. Eng.*, 19: 371-399.
- Rigo, M.L. 2006. The residual shear strength of tropical soils. *Canadian Geotechnical Journal*, 43(4): 431-447.
- Saito, H. et al. 2010. Relationship between the initiation of a shallow landslide and rainfall intensity—duration thresholds in Japan. *Geomorphology*, 118: 167-175.
- Stark, T.D. and Vettel, J.J. 1992. Bromhead ring shear test procedure. *Geotechnical Testing Journal*, 15: 24-32.
- Tohari, A. et al. 2007. Laboratory rainfall-induced slope failure with moisture content measurement. *J. Geotech. and Geoenv. Eng.*, 133(5): 575-587.
- Zhou, C.H. et al. 2002. On the spatial relationship between landslides and causative factors on Lantau Island. Hong Kong. *Geomorphology*, 43: 197-207.
- Van Asch, T.W.J. et al. 1999. A view on some hydrological triggering systems in landslides. *Geomorphology*, 30: 25-32.